Journal of Applied Sciences

ISSN 1812-5654

Journal of Applied Sciences 11 (10): 1845-1850, 2011
ISSN 1812-5654 / DOI: 10.3923/jas.2011.1845.1850

Burst Strength Analysis of Corroded Pipelines by Finite Element Method

Chanyalew T. Belachew, Mokhtar C. Ismail and S. Karuppanan
Department of Mechanical Engineering, Universiti Teknologi PETRONAS, Bandar Seri Iskandar, 31750 Tronoh, Perak, Malaysia

Abstract: Corrosion has become one of the main threats towards maintaining pipeline's integrity. At the point of corrosion, the wall of the pipe becomes thinner and starts to lose its mechanical resistance. Methods for assessing metal loss defects have been available for many decades, as for instance the NG-18 equation and ANSI/ASME B31G code. Throughout the years many modifications to the original equations have been made and newer methods like Modified B31G and RSTRENG were adopted. These days, several in-house methods and commercial codes are available but they are known to be conservative. Therefore, pipeline operators need reliable defect assessment methodology not only to assure safe operation but also to implement optimum operation cost. Based on these motivations, in the recent years various alternative methods have been developed mostly based on finite element studies and burst tests. This study presents the application of nonlinear finite element analyses for burst strength analysis of corroded pipe.

Key words: Pipeline assessment, nonlinear analysis, burst pressure

INTRODUCTION

Failure due to corrosion has been one of the greatest concerns in maintaining the pipelines integrity. As the pipeline infrastructure ages, metal loss due to corrosion represents a major source of material degradation in steel pipes which most often reduces its burst strength with increased potential for catastrophic failure. Corrosion is a time dependent electrochemical process and depends on the local environment within or adjacent to the pipeline (Cosham and Kirkwood, 2000). At the points where corrosion occur the wall of the pipe become thinner, leading to loss of its mechanical resistance. Therefore, the continual service of corroded pipelines must be guaranteed by Fitness-for-service (FFS) assessments.

FFS decisions are made based on prediction of the residual strength of the corroded pipeline (Escoe, 2006). Methods for assessing corrosion metal loss defects have been available for many decades, as for instance the NG-18 equation and ANSI/ASME B31G code. Throughout the years many modifications were made to the original equations and many newer methods like ASME B31.G (ANSI/ASME, 1991), Modified B31G (KAPA, 2000), RSTRENG (Kiefner, 2006), DNV RP-F101 and several in-house codes were adopted.

Although, these widely used acceptance criteria simplify the integrity assessments of in-service pipelines, they are known to be conservative (Belachew *et al*., 2009a) and thus enforce premature retirement of pipelines. Therefore, pipeline operators need reliable defect assessment method not only to assure safe operation but also to implement optimum operation cost. Motivated by these observations, in the recent years various alternative assessment methods have been developed mostly based on finite element studies and burst test results.

Modern numerical analysis methods have enabled the modelling of realistic defect shapes and nonlinear material behaviour (Lee and Kim, 2000). Conventional procedures used to assess the integrity of corroded piping systems with axial defects generally employ simplified failure criteria based upon a plastic collapse failure mechanism incorporating the tensile properties of the pipe material (Chiodo and Ruggieri, 2009). In this paper the finite element simulation of various corrosion defects are presented. A central focus is to gain insight into the effects of defect depth, defect extent and defect width on the burst strength of the pipeline. Stress-based criterion based on plastic instability analysis was used to predict the failure pressure (Belachew *et al*., 2009b). During the simulation of nonlinearities due to plastic-deformation and large-deformation were considered. The results were compared with the predicted burst pressures using some of the commercial codes.

Consideration of nonlinearities: During failure simulation the pipeline materials are subject to irreversible structural

Corresponding Author: Chanyalew T. Belachew, Department of Mechanical Engineering, Universiti Teknologi PETRONAS, Bandar Seri Iskandar, 31750 Tronoh, Perak, Malaysia

deformation due to loading beyond the material's yielding point. Therefore, the nonlinear stress-strain relationship and the changes in geometry due to large displacements require a nonlinear structural analysis. These structural nonlinearities are usually know as material-and geometric- nonlinearities. The geometrical nonlinearity is associated with the necessity to updating the coordinates of the initial and final states of deformations during the finite element simulations. True stress and true strain material properties based on incremental plasticity approach is used expression the material properties (ANSYS, 2009).

To accurately predict the behaviour of a corrosion defect, the material behaviour, in particular the plastic behaviour must be modelled appropriately. The finite element model allows the material behaviour to be modelled with a uniaxial true stress-strain curve as mentioned in Fig. 1. The use of true-stress versus true-strain data allows an incremental plasticity scheme to be used which can account for strain hardening and subsequent unloading, but requires a significant increase in computing resources (Chouchaoui, 1993). If the stresses increase monotonically and significant unloading does not occur, the stress-strain behaviour of typical pipeline materials can be modelled with deformation plasticity theory using the Ramberg-Osgood Eq. 1 to represent the true stress-strain curve (Ramberg and Osgood, 1943):

$$\varepsilon=\frac{\sigma}{E}+\alpha\left(\frac{\sigma}{\sigma_y}\right)^{n-1}\frac{\sigma}{E} \tag{1}$$

Pipeline steels typically display anisotropic yield behaviour as a result of the rolling process used to create the steel plate from which the pipe is manufactured. For the analysis of corroded pipe, it is recommended to use the material properties in the circumferential direction since this is the direction of maximum principal stress in plain pipe (Chouchaoui and Pick, 1996).

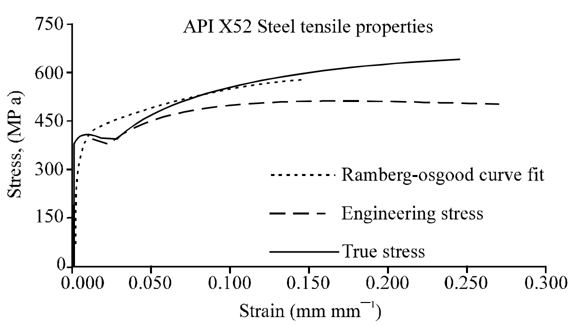

Fig. 1: Tensile properties of the API X52 grade steel (DNV, 1997)

FINITE ELEMENT METHOD

Analysis procedures: The solution to the nonlinear governing equations can be achieved through an incremental approach. The incremental form of the governing equations can be written as shown in Eq. 2 (Zienkiewicz, 1971):

$$K(u)\Delta u=\Delta P \tag{2}$$

where, Δu is unknown incremental displacement vector, is ΔP unknown incremental applied load vector.

The solution is obtained by taking a series of linear steps in the appropriate direction in order to closely approximate the exact solution. When solving nonlinear problems, ANSYS® uses the Newton-Raphson (N-R) method, which involves an iterative procedure. This method starts with assumed solution and determines the magnitude of the increment as mentioned in Eq. 3 and 4, respectively. The corresponding out-of-balance load vector, which is the difference between the applied loads and the loads evaluated based on the assumed solution is calculated as enlisted in Eq. 5:

$$u=u_i \tag{3}$$

$$\Delta u_i=K^{-1}(u_i)\Delta P \tag{4}$$

$$\Delta R_i=\Delta P-K(u_i)\Delta u_i \tag{5}$$

In order to satisfy the equilibrium conditions exactly, the out-of-balance load vector must be zero. However, as the nonlinear equilibrium conditions are solved approximately, a tolerance is introduced for the out-of-balance load vector in order to terminate the solution procedure. In each iterations, the N-R method computes the out-of-balance load vector and checks for convergence based on the specified tolerance. If the convergence criterion is not satisfied, the trial solution is updated and based on the calculated incremental displacements, the next incremental solution vector is determined as dipict in Eq. 6 and 7 leading to the computation of the new out-of-balance load vector as mentioned in Eq. 8:

$$u_{i+1}=u_i+\Delta u_i \tag{6}$$

$$\Delta u_{i+1}=K^{-1}(u_{i+1})\Delta P \tag{7}$$

$$\Delta R_{i+1} = \Delta P - K(u_{i+1})\Delta u_{i+1} \quad (8)$$

This procedure is repeated until convergence is accomplished. There are also options like time stepping, a bisection method and line search algorithm methods for improving the convergence in ANSYS®.

Element type: In this study, higher order 8-node solid elements (SOLID45) were used to analyse the 3D models. Accurate application of the finite element method involves the use of a large number of 3D solid elements to correctly model the corrosion geometry and the use of large displacement, elastic-plastic analysis to model the material response (Cronin, 2000; Szary, 2006). Two layers of elements were used through the remaining ligament of each corrosion defect. The element type chosen allows both material non-linearity and large localized non-linear deformation to be performed (ANSYS, 2009).

Boundary conditions and loading: The symmetries of boundary conditions, as mentioned in Fig. 2, were used in order to reduce the size of the models and hence reduce computer run times. Coarser meshes are used farther from the defect location to reduce the nodes number. Constraints were also applied to the models to eliminate rigid body motion. The model was extended far enough from the defect location to ensure the boundary conditions did not affect the results of the analyses. Internal pressure loading was applied to each model and automatically increased during the FE analysis. Tensile axial loads were applied at the ends of the pipe in order to simulate the end-caps during burst test.

Failure criteria: Failure may be defined as a limit above which material fails. It may occur as a fracture, excessive deformation or when an arbitrary set value of stress, strain or energy is reached. Corrosion defects are relatively smooth and pipe materials are generally tough, therefore, the failure of the corrosion defect is usually by plastic collapse of the defect ligament as opposed to low ductile fracture (Chouchaoui, 1993). Observations of the corroded material in the vicinity of the failures show a significant amount of plastic deformation and localized necking indicating that the initial failure occur by plastic collapse. The contours of the grain structure in the vicinity of the failure show a significant localization of the deformations at the failure location (Cronin and Pick, 2002).

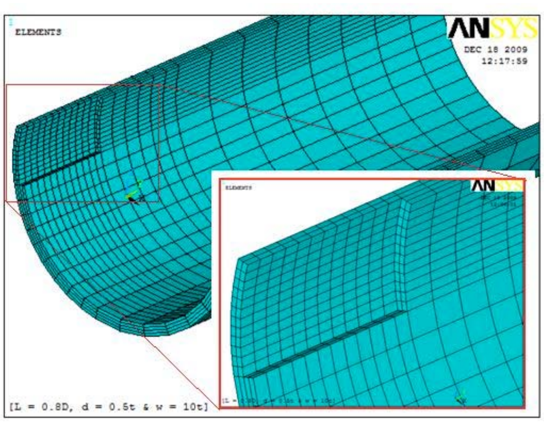

Fig. 2: Finite element model of the defect and mesh close view

Finite element analysis of pipe with corrosion defects do not in itself predict the failure pressure of the pipe since it is impossible to predict local instability, such as necking, which usually leads to ultimate failure. Thus, there should be defined criterion to decide the failure point during simulation. In this work, the two-criterion approach, stress-based and instability based criteria was used to locate the failure points (Chouchaoui, 1993). This approach involves the calculation of a critical stress or strain value according to the stress-strain curve of the material. Plastic collapse is deemed to occur either when the equivalent stress exceeded the critical stress through the entire thickness of the ligament or when the gradient of plastic strain through the entire ligament becomes constant and the plastic strain increase asymptotically.

The critical stress is defined as the ultimate tensile stress from the true stress-strain relationship. Among the different failure theories ANSYS® uses the von Mises criterion. For pipe calculation it is more convenient to use this theory with cylindrical coordinates, where stress components are combined into one effective stress as enlisted in Eq. 9:

$$\sigma_e = \frac{1}{2}\sqrt{(\sigma_\theta - \sigma_r)^2 + (\sigma_\theta - \sigma_L)^2 + (\sigma_r - \sigma_L)^2} \quad (9)$$

Where:

σ_L : Axial stress

σ_θ : Tangential (hoop) stress

σ_r : Radial stress

σ_e : Equivalent (von Mises) stress

RESULTS AND DISCUSSION

The models were developed from API X52 steel with nominal dimensions of 274 mm diameter, 12 mm wall thickness and 600 mm section length. These models were selected to cover the following basic parameters: normalized defect depth (d/t of 0.10, 0.20, 0.40, 0.50, 0.60, 0.75, 0.80 and 0.90, normalized defect extent (L/D of 0.20, 0.40, 0.60, 0.80, 0.94, 1.00, 1.20, 1.40, 1.60, 1.80 and 2.0 and normalized corrosion width (w/t of 1.0, 2.0, 3.0, 5.0, 10.0 and 15.0). For the full matrix of the pipe and defect dimensions given above, a total of 29 models with internal defect were generated. One more model with an external defect was developed to compare the effect of similar defects on the external and inner surface of the pipeline. For convenience all the predicted failure pressure is normalized with the failure pressure of an intact pipe according to maximum hoop stress theory as mentioned in Eq. 10:

$$p_{max} = \frac{2t}{D-t}\sigma_{UTS} \tag{10}$$

With the increase of internal pressure, the stress variation through the ligament exhibits three distinct stages; elastic deformation, plastic deformation and material hardening. This phenomenon is justified by various researchers (Fu and Kirkwood, 1995, Choi *et al*., 2003, Lee and Kim, 2000. The stress distribution through the ligament is dipicted in Fig. 3.

- **Elastic deformation:** A linear response progressing to a point when the elastic limit is reached
- **Plastic deformation:** Plasticity spreads through the ligament (the von Mises equivalent stress increases very slowly because of the constraint of the surrounding pipe wall)
- **Material hardening:** The whole of the ligament deforms plastically but failure does not occur because of material work hardening. Failure of the defect pipe was deemed to occur when the minimum von Mises equivalent stress in the ligament was equal to the true ultimate tensile strength of the material. At this stage the plastic strain increases drastically as drawn in Fig. 4, which confirms structural instability

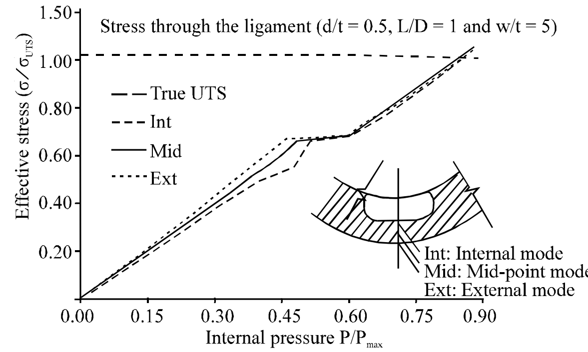

Fig. 3: Von Mises stress distribution through the ligament

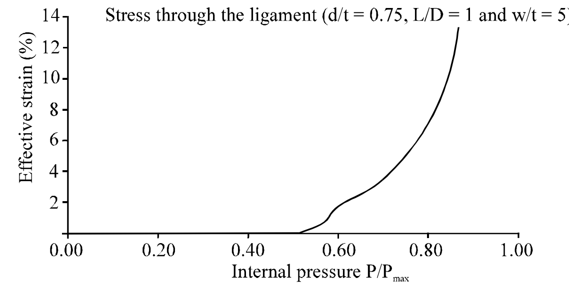

Fig. 4: Von mises plastic strain distribution through the ligament

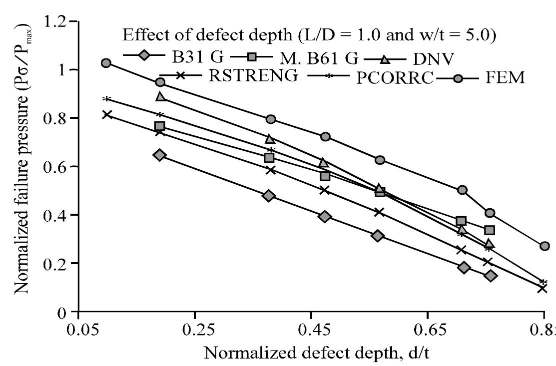

Fig. 5: Effect of defect depth on burst strength

Figure 5 illustrates the effect of defect depth on the burst strength by using four commercial codes and FEM. As the defect depth increase, the burst strength decrease. The predictions by the commercial codes showed conservative estimation brust of the strength. On average deviation of 44% for B31 G, 21% for Modified B31 G, 16% for DNV, 31% for RSTRENG and 21% for PCORRC were observed as compared to the FE results.

Figure 6 illustrates the effect of longitudinal extent of the defect on the burst strength by using four commercial codes and FEM. As the defect length increases up to about the size of nominal diameter, the burst pressure Nov. 3, 2010 decreases. Further increase of the defect length has insignificant effect on the burst strength. Similarly, the commercial codes showed conservative estimation. On average deviation of 33% for B31 G, 19% for Modified B31 G, 11% for DNV, 27% for RSTRENG and 17% for PCORRC were observed as compared to the FE results.

Figure 7 illustrates the effect of defect width on the burst strength of pipelines using FE simulation. It was observed that a defect width more than four times the

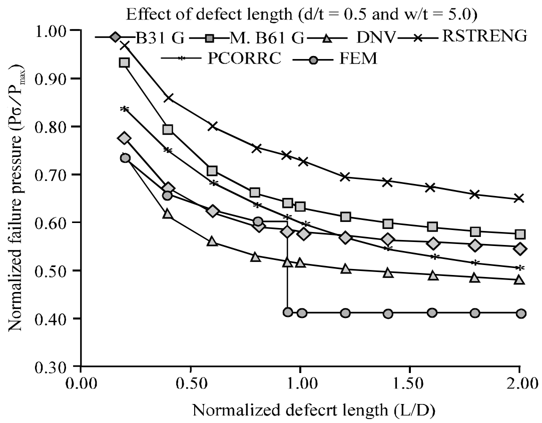

Fig. 6: Effect of defect extent on burst strength

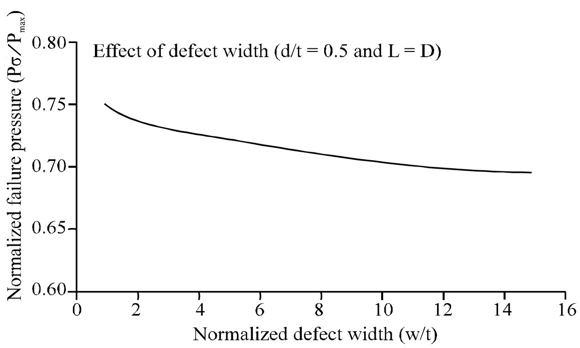

Fig. 7: Effect of defect width on burst strength

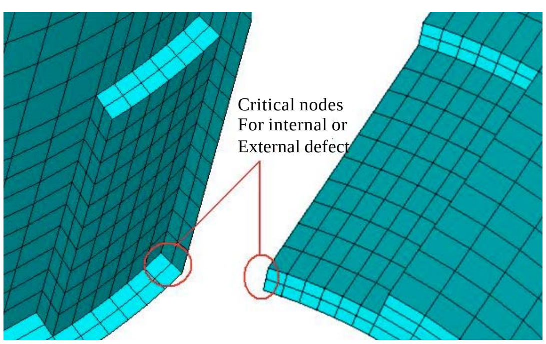

Fig. 8: Effect of equivalent defect on the internal or external surface

nominal wall thickness has insignificant effect on the burst strength. Therefore, the fact that excluding the effect of circumferential extent of the defect in commercial codes is justifiable for defects wider than four times the nominal thickness of the pipe.

The effect of equivalent defect located on external and internal surface of the pipe were evaluated for the critical nodes as shown in Fig. 8. The von Mises plastic

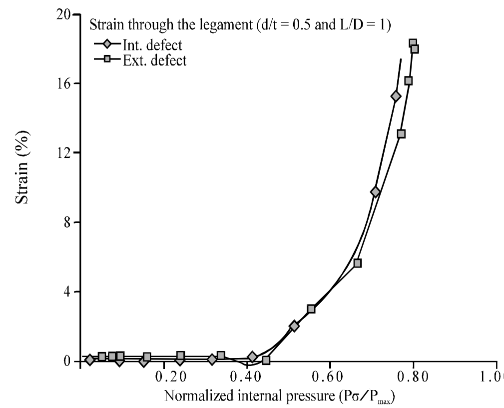

Fig. 9: Von Mises plastic strain distribution through the ligament

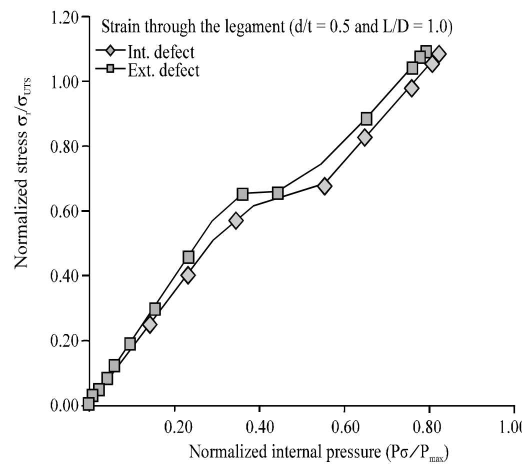

Fig. 10: Von Mises stress distribution through the ligament

strain and von Mises stress distribution through the ligament is shown in Fig. 9 and 10, respectively. The result certify that, the location of the defect have no significant effect on the burst strength analysis.

CONCLUSION

Simulation results of various corrosion defects were presented. The effects of defect depth, defect longitudinal and circumferential extent on the burst strength of the pipeline were studied. Stress-based criterion based on plastic instability analysis was used to predict the failure pressure. During the FE simulation the nonlinearities due to plastic-deformation and large-deformation were considered. The results were compared with the predicted burst pressures using some of the available commercial codes. The following observations were forwarded:

- Available commercial codes for pipeline capacity assessment are conservative
- As the defect depth increase, the burst strength of the pipe decrease more or less in a linear manner
- The effects of an infinitely extended longitudinal defect can be approximated by an equivalent defect length equal to pipeline nominal diameter
- The effects of circumferentially extended defect more than four times the pipeline nominal thickness can be approximated as defect having width equal to four times the nominal pipeline wall thickness
- Circumferential extent of defect less than two times the nominal pipeline wall thickness need special attention due to excessive stress concentration
- Equivalent defect on the internal or external surface of the pipe have approximately similar effect on the burst strength of the pipe

REFERENCES

ANSI/ASME, 1991. Manual for Determining the Remaining Strength of Corroded Pipelines: A supplement to ASME B31 Code for Pressure Piping. American Society of Mechanical Engineers, USA., pp: 55.

ANSYS, 2009. ANSYS, Release 12.0 Documentation for ANSYS. SAS IP, Inc., Canonsburg, PA.

Belachew, C.T., M.C. Ismail and K. Saravanan, 2009a. Capacity assessment of corroded pipelines using available codes. NACE Asis Pacific, Kuala Lumpur. http://eprints.utp.edu.my/1772/1/NACE_Conference_Paper.pdf.

Belachew, C.T., M.C. Ismail and K. Saravanan, 2009b. Effect of corrosion defect on burst pressure of pipelines: Numerical studies and validation. Proceedings of the NACE East Asian and Pacific Regional Conference and Exposition, Kuala Lumpur, Malaysia.

Chiodo, M.S.G. and C. Ruggieri, 2009. Failure assessments of corroded pipelines with axial defects using stress-based criteria: Numerical studies and verification analyses. Int. J. Pressure Vessels Piping, 86: 164-176.

Choi, J.B., B.K. Goo, J.C. Kim, Y.J. Kim and W.S. Kim, 2003. Development of limit load solutions for corroded gas pipelines. Int. J. Pressure Vessels Piping, 80: 121-128.

Chouchaoui, B., 1993. Evaluating the remaining strength of corroded pipelines. Ph.D. Thesis, Department in Mechanical Engineering, University of Waterloo, Canada.

Chouchaoui, B.A. and R.J. Pick, 1996. Behaviour of longitudinally aligned corrosion pits. Int. J. Pressure Vessels Piping, 67: 17-35.

Cosham, A. and M. Kirkwood, 2000. Best practice in pipeline defect. Proceedings of the International Pipeline Conference, Oct. 2000, Calgary, Alberta, Canada, pp: 1-12.

Cronin, D.S. and R.J. Pick, 2002. Prediction of the failure pressure for complex corrosion defects. Int. J. Pressure Vessels Piping, 79: 279-287.

Cronin, D.S., 2000. Assessment of corrosion defect in pipelines. Ph.D. Thesis, University of Waterloo, Canada.

DNV, 1997. Reliability of corroded pipes finite element analyses. Report No. 96-3392, Revision No. 01, Hovik, Norway.

Escoe, K., 2006. Piping and Pipelines Assessment Guide. 1st Edn., Gulf Professional Publishing, USA., ISBN-13: 978-0750678803, pp: 560.

Fu, B. and M.G. Kirkwood, 1995. Predicting failure pressure of internally corroded linepipe using the finite element method. OMAE V Pipeline Technology: ASME, 1995.

KAPA, 2000. A Modified Criterion for Evaluating the Remaining Strength of Corroded Pipe. Kiefner and Associates Inc., Worthington, OH, USA.

Kiefner, 2006. KAPA 2006. Kiefner and Associates Inc., Worthington, Ohio.

Lee, O.S. and H.J. Kim, 2000. Effect of external corrosion in pipeline on failure prediction. Int. J. Korean Soc. Precision Eng., 1: 48-54.

Ramberg, W. and W.R. Osgood, 1943. Description of stress-strain curves by three parameters. Technical Note,Washington.http://www.apesolutions.com/spd/public/NACA-TN902.pdf.

Szary, T., 2006. The finite element method analysis for assessing the remaining strength of corroded oil field casing and tubing. Ph.D. Thesis, Department of Mechanical Engineering, Germany.

Zienkiewicz, O.C., 1971. The Finite Element Method in Engineering Sciences. McGraw Hill, London.